The International Supercritical CO_2 Energy Technologies Symposium
March 2 - 5, 2026, Pittsburgh, PA
Paper #033

Oxidation of Materials and Coatings at 1000 °C and 250 bar for use in Oxy-Combustion Turbine

Florent Bocher
Senior Research Engineer
Southwest Research Institute
San Antonio, TX, USA

Jeffrey Moore
Institute Engineer
Southwest Research Institute
San Antonio, TX, USA

Michael Marshall
Research Engineer
Southwest Research Institute
San Antonio, TX, USA

Insert author(s) Bio and Photo here

Dr. Florent Bocher is a Senior Research Engineer at Southwest Research Institute in San Antonio, Texas. He has a "Diplôme d'Ingénieur" in materials engineering from ESSTIN, France (now École Polytechnique de l'Université de Lorraine) and a Ph.D. in Materials Science from Imperial College, UK. He specializes in studying environmental performance of materials, including corrosion of metallic alloys and degradation of elastomers and polymers. He has led dozens of R&D projects on evaluating materials in high-temperature and/or high-pressure environments found in various industries such as nuclear power generation, upstream oil and gas, biofuel refinement, hydrogen diffusion, energy generation, and chemical processes.

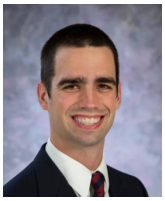

Michael Marshall is a Research Engineer in the Machinery Department at Southwest Research Institute, where he has conducted work on a range of sCO2 power cycle applications. He earned his Bachelors in Aerospace Engineering in 2018 from the University of Virginia. His experience includes experimental heat transfer testing, turbomachine and heat exchanger design, root cause failure analysis, and thermodynamic cycle modeling.

Dr. Jeffrey Moore is an Institute Engineer in the Machinery Section at Southwest Research Institute in San Antonio, TX. He holds a B.S., M.S., and Ph.D. in Mechanical Engineering from Texas A&M University. His professional experience over the last 30 years includes engineering and management responsibilities related to centrifugal compressors and gas turbines at Solar Turbines Inc. in San Diego, CA, Dresser-Rand (now Siemens Energy) in Olean, NY, and Southwest Research Institute in San Antonio, TX. His interests include advanced power cycles and compression methods, rotordynamics, seals and bearings, computational fluid dynamics, finite element analysis, machine design, controls, aerodynamics, and oxy-combustion. He has authored over 40 technical papers related to turbomachinery and has four patents issued. Dr. Moore has held positions as the Vanguard Chair of the Structures and

Dynamics Committee and Chair of Oil and Gas Committee for IGTI Turbo Expo. He has also served as the Associate Editor for the Journal of Tribology and a member of the IGTI sCO_2 Committee, Turbomachinery Symposium Advisory Committee, the IFToMM International Rotordynamics Conference Committee, and the API 616 and 684 Task Forces.

ABSTRACT

Combinations of materials and coatings were tested in supercritical CO_2 (sCO_2) to evaluate their reliability in an oxy-fuel turbine being designed to operate in the 150-300 MWe size range at inlet temperatures of 1,150 °C at 300 bar and exhaust temperatures in the 725-775 °C range.

Nickel alloys and stainless steels were exposed to supercritical CO_2 at 1,000 °C and 250 bar for a total of over 1,500 hours. The materials were tested bare, with a nanocrystalline MCrAlY bond coat only, or with one of two types of bond coat and a thermal barrier coating. A novel test facility using a localized heat zone generated by an induction heater inside an externally cooled autoclave was developed to perform those tests. The specimens were weighed before and after exposure to determine the oxidation rate. All specimens were inspected visually, and a smaller group of coated specimens were studied using secondary electron microscopy (SEM). The integrity of the coating, and the morphology and composition of the thermally grown oxide were especially of interest for the SEM investigation.

This paper presents the up-to-date results of the testing coated and uncoated superalloys in sCO_2 at up to 1150 °C and up to 300 bar performed at Southwest Research Institute.

INTRODUCTION

Project Background

Competitive plant efficiencies may be achieved using direct-fired sCO_2 power cycles featuring oxy-combustion, making it an attractive technology. These cycles may also be capable of near zero CO_2 emissions. Past system studies on the Allam-Fetvedt cycle predicted a 53% LHV net efficiency for a plant utilizing natural gas,[1] and a 42% LHV net efficiency for a plant utilizing coal syngas fuel.[2]

The oxy-combustion systems rely on turbines with inlet temperatures exceeding 1,100 °C. The design undertaken as part of the project sponsored by the U.S. Department of Energy (FE-0031929) includes a six-stage turbine with an input temperature of 1,150 °C at nearly 300 bar.[3] A schematic of the turbine and the design temperatures and pressures are presented in Figure 1. As part of this project the various materials considered for the turbine are being evaluated in CO_2 at up to 1,150 °C. The materials evaluation process includes thermal cycling at ambient pressure CO_2 and long term autoclave testing in high pressure and high temperature sCO_2. Oxidation and thermal management coatings are also included in the experimental matrix.

The materials decision and presentation of the long term autoclave testing facility are presented in this paper along with some of the up-to-date achievements and design optimization.

a. 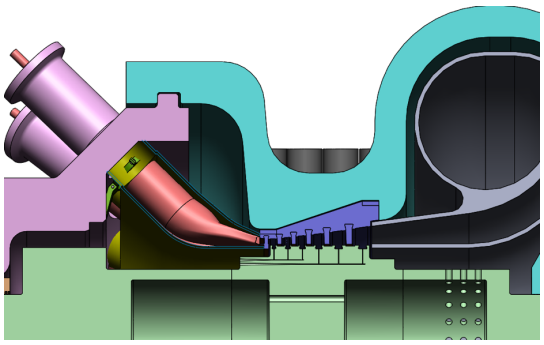 b. 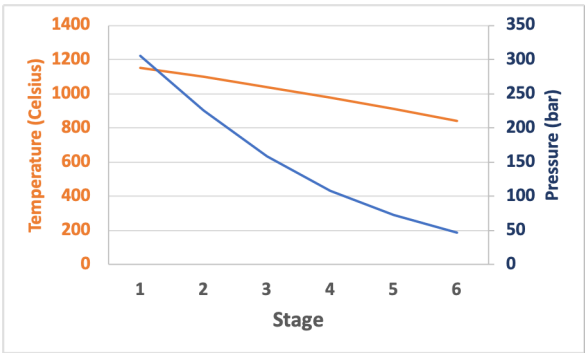

Figure 1. a. Schematic of the six-stage turbine and b. design pressures and temperatures across the stages.

RESULTS AND DISCUSSION

Materials and Specimens

A total of six alloys were included in this study. They included nickel alloys and stainless steels that have previously been considered for this application and include Inconel 625 as a baseline alloy that has been evaluated in supercritical CO_2 in multiple studies.[4–13] All alloys were exposed with or without a nanocrystalline MCrAlY bond coat. Three of the alloys (740H, 282, and 625) were also tested with nanocrystalline bond coat and thermal barrier coating (TBC) or with a thermal spray bond coat and TBC. The TBC was an yttria-stabilized zirconia-based coating. The list of materials, UNS number, description, and their treatments are summarized in Table 1.

The specimens were machined to a dimension of approximately 1 cm × 1 cm × 0.15 cm, with two 1.5 mm holes. The specimens were coated after machining. Photographs of coated and uncoated 282 specimens are showed in Figure 2 as an example. The nanocrystalline bond coat was approximately 50 μm thick and thus difficult to visually observe. However, specimens with TBC were obviously thicker. The TBC was white and had a porous appearance. All specimens were measured (down to 10^{-4} inch), photographed, and weighed three times down to 0.01 mg.

Table 1. List of alloys included in the study, with their UNS number and description. Quantity of each alloy either bare, with a nanocrystalline bond coat alone (NC BC), a nanocrystalline bond coat and thermal barrier coating (NC BC & TBC), or a thermal spray bond coat and thermal barrier coating (TS BC & TBC). Mass change analysis will be performed on all specimens. Additionally, SEM will be performed on the specimens with TBC.

Alloy	UNS	Description	Bare	NC BC	NC BC & TBC	TS BC & TBC
740H	N07740	Age hardened chromia former nickel alloy	3	3	3	3
625	N06625	Baseline nickel-chromium alloy	3	3	3	3
282	N07208	Wrought, gamma-prime strengthened nickel superalloy	3	3	3	3
APMT Kanthal	n/a	Dispersion strengthened ferritic iron-chromium-aluminum alloy	3	3	-	-
353 MA	S35315	Austenitic, chromium-nickel stainless steel	3	3	-	-
Sanicro 25	S31035	Austenitic 22Cr25NiWCoCu stainless steel	3	3	-	-

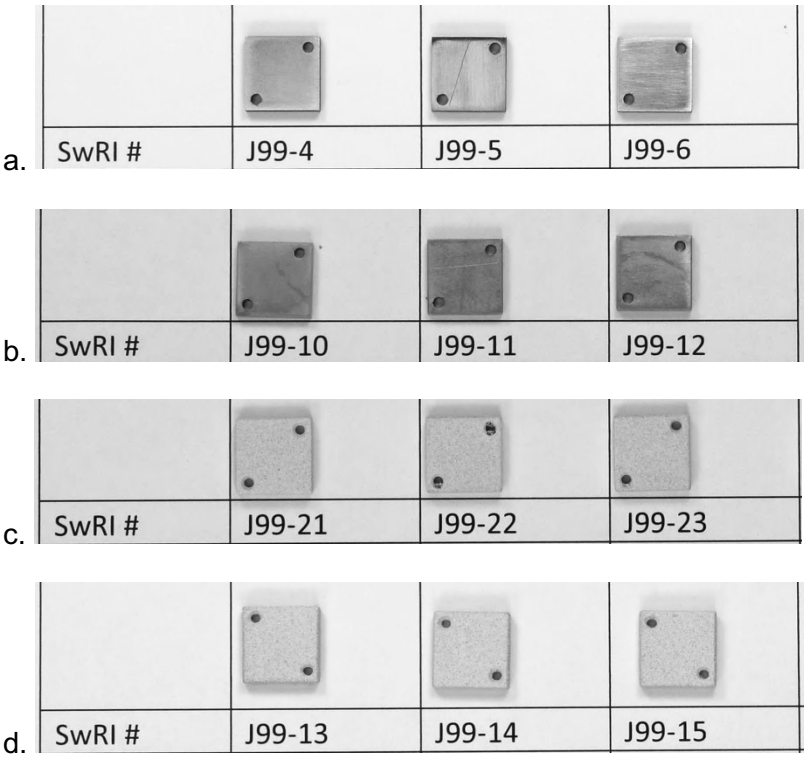

Figure 2. Photographs before exposure of alloy 282 specimens a. bare, b. with nanocrystalline MCrAlY bond coat, c. with nanocrystalline MCrAlY bond coat and TBC, and d. with thermal sprayed bond coat and TBC.

Testing Facility

A unique testing facility was designed using an induction heater to test materials at up to 1,150 °C and 300 bar. High pressure and high temperature material tests are usually performed using autoclaves that are externally heated using electrical heaters or furnace. The autoclaves must be rated for the test pressure at the test temperature. The new test facility relies on putting the heating source inside the pressurized vessel. Temperatures exceeding 1,000 °C can be achieved locally while the pressure vessel remains below its 350 °C rating. This setup uses an induction heater in a 4-liter stainless steel autoclave. A schematic of the setup is presented in Figure 2. The induction coil was placed inside the autoclave to create a localized heat zone. The inner wall of the autoclave was isolated from the heat zone by using insulation wrapped in stainless steel. The specimens were located outside of the coil to avoid heating coated samples from the inside out. They were placed in a specimen holder made of stainless steel 310, shown in Figure 3. The middle part of the holder acted as a susceptor and was surrounded by the induction coil. The specimens were placed in holes on the top and bottom of the holder, which were outside of the induction coil. The material surrounding the specimens heated by heat diffusing from the susceptor. This created a very high temperature environment in the holes without heating the specimen by induction. Lids were added to the top and bottom to keep hot sCO_2 in this enclosed environment. Vent holes were placed on the side of the specimen holder. They were used to maintain a pressure equilibrium and to place thermocouples in the environment near the specimens.

The autoclave was placed upside down during the test in order to keep the densest and coolest sCO_2 near the head of the autoclave where the most temperature-sensitive parts of the autoclave (e.g. fittings, seal, coil connection) were. This was done to reduce chances of failures. The power compression seal feedthroughs, used to pass the copper tube connected to the coil, had to be actively cooled using a custom-made chilling jacket (shown in the middle left photograph in Figure 2). The power of the induction heater was regulated using two thermocouples placed in and near the heat zone, which were connected to the induction heater. One thermocouple type S was placed nearest to the specimens and was the reference for test temperature (later referred as “high temperature”). A thermocouple type K was placed in the vent hole to measure the temperature of the specimen holder (later referred as “mid temperature”).

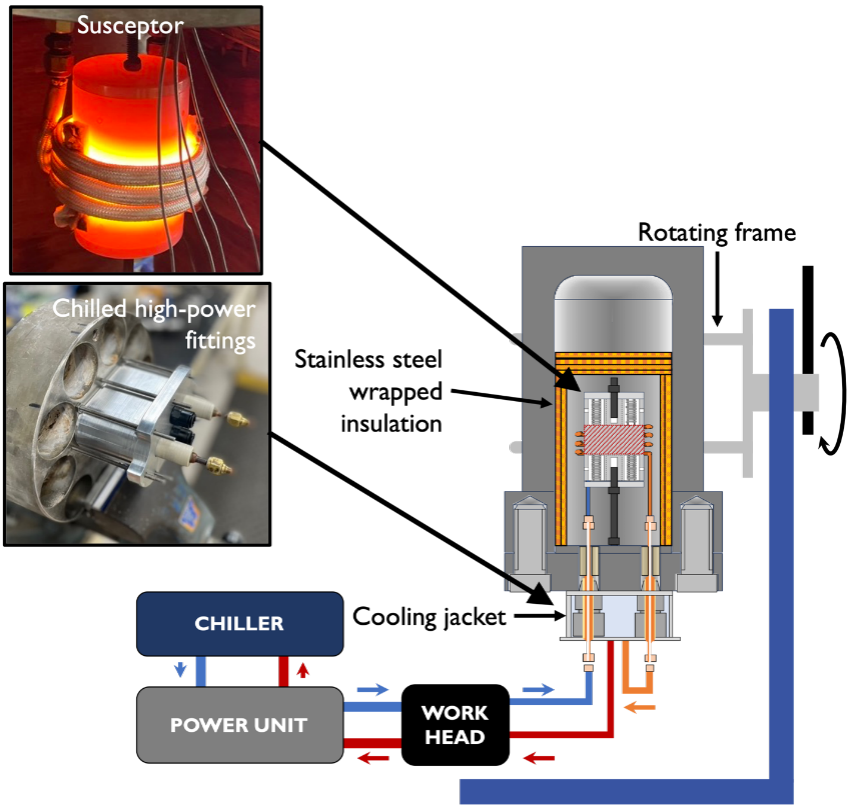

Figure 2: Schematic of induction heater in autoclave used to test materials at temperature exceeding 1,000 °C and at pressure up to 300 bar

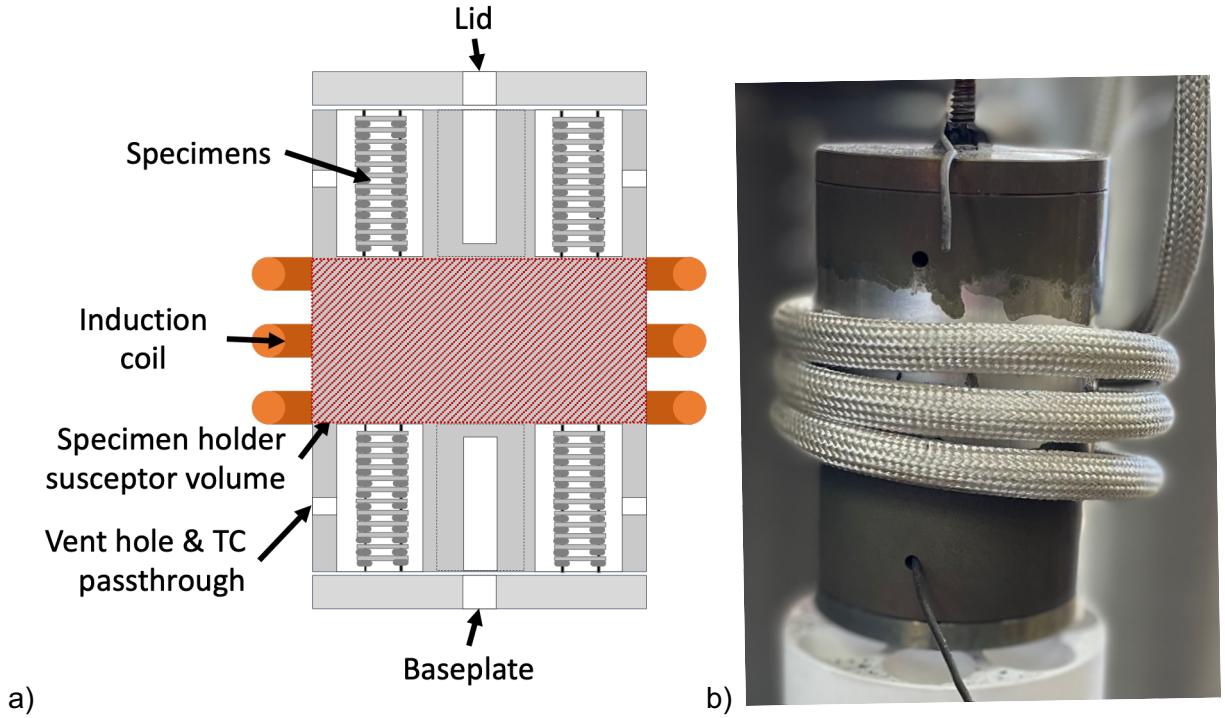

Figure 3. a) Cross sectional schematic and b) photograph of the optimized design of the specimen holder/susceptor assembly inside an induction coil (in orange).

Test Description

A total of 54 coupons, described in Table 1, were exposed to sCO_2 for a total of 1,500 hours, during three 500 hours experiments. The coupons were weighed three times using a scale with 0.01 mg accuracy before exposures. They were weighed once with the same scale after each exposures. The coupons were also photographed before and after exposures.

Results

The temperature and pressure data measured during the three 500 hours exposures are presented in Figure 4, Figure 5, and Figure 6.

Test temperature and pressure quickly reached 1,000 °C and 4,000 psi during the first exposure. A small leak started at one of the induction heater fitting after 75 hours. The autoclave was regularly refilled with CO_2 to maintain the pressure above the critical point. The induction heater shut off after nearly 90 hours for approximately 10 hours. During that time the temperature went down to less than 200 °C and the pressure reached 1,000 psi. The temperature and pressure increased again once the induction heater was restarted. The high temperature remained near 1,000 °C during the whole test. Post mortem evaluation revealed that one of the compression seal feedthroughs was the cause of the slow leak. The feedthrough was replaced before starting the second test.

Before the second test, the mid temperature thermocouple was also adjusted to better measure the temperature specimen holder. The temperature remained near 1,000 °C for the entirety of the second test. The pressure fluctuated around 3,500 psi. The frequency of the pressure oscillation was 24 hours and was due to daily temperature fluctuation. The induction heater was slowly cooled down to avoid thermal shocks that may damage the setup. The insert in Figure 5 shows the 100 °C per hour controlled cooling at the end of the project.

During the third test, the thermocouple for the high temperature stopped working at 500 °C, as can be seen in the insert of Figure 6. The mid temperature was therefore used to monitor the test conditions. In order to choose the mid temperature to be maintained during test 3, the high temperatures were plotted against the mid temperatures, see Figure 7. The measured temperatures were plotted and logarithmic fits were used to determine what the mid temperatures would be when the high temperatures were 1,000 °C. This method was validated by using the data from test 2. The calculated mid temperature for the second exposure was 600 °C, as observed during the test. Using this method, it was decided to set the mid temperature to 650 °C during test 3, so the temperature of the specimens would be close to 1,000 °C.

The average and standard deviation of the high and mid temperatures during the three tests are summarized in Table 2. It is notable that the standard deviations are smaller for tests 2 and 3 than for test 1. This is because the maximum power of the induction heater had been reduced, which provided a more stable system.

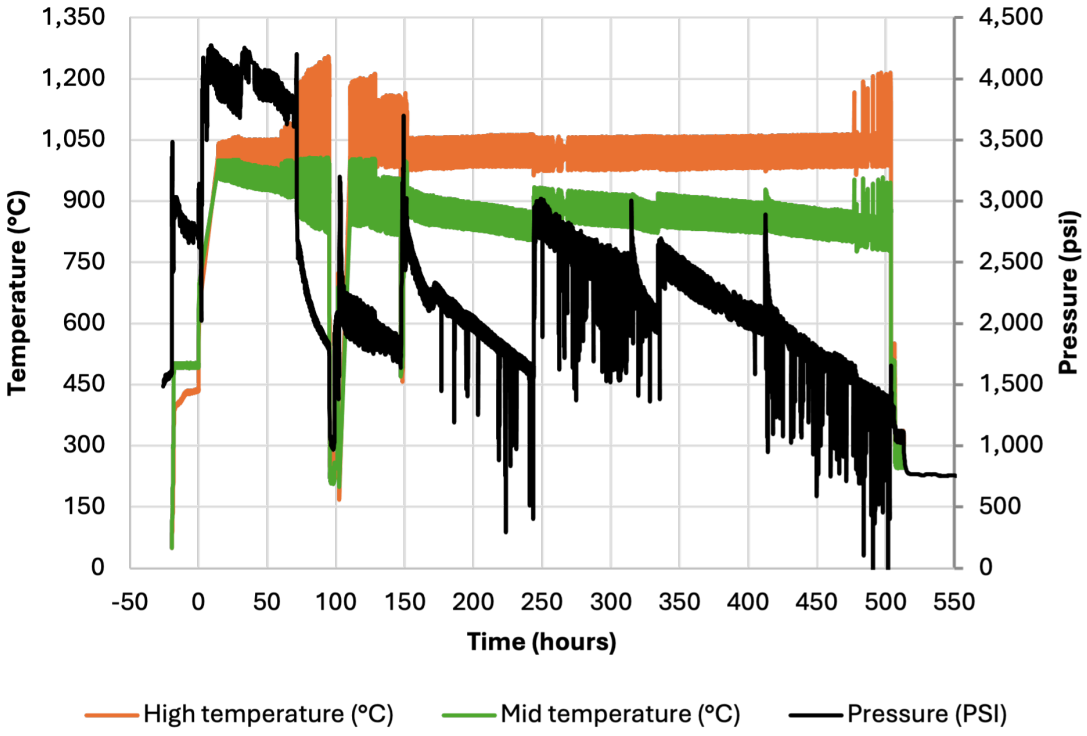

Figure 4. Measured temperature and pressure during the first 500 hours exposure.

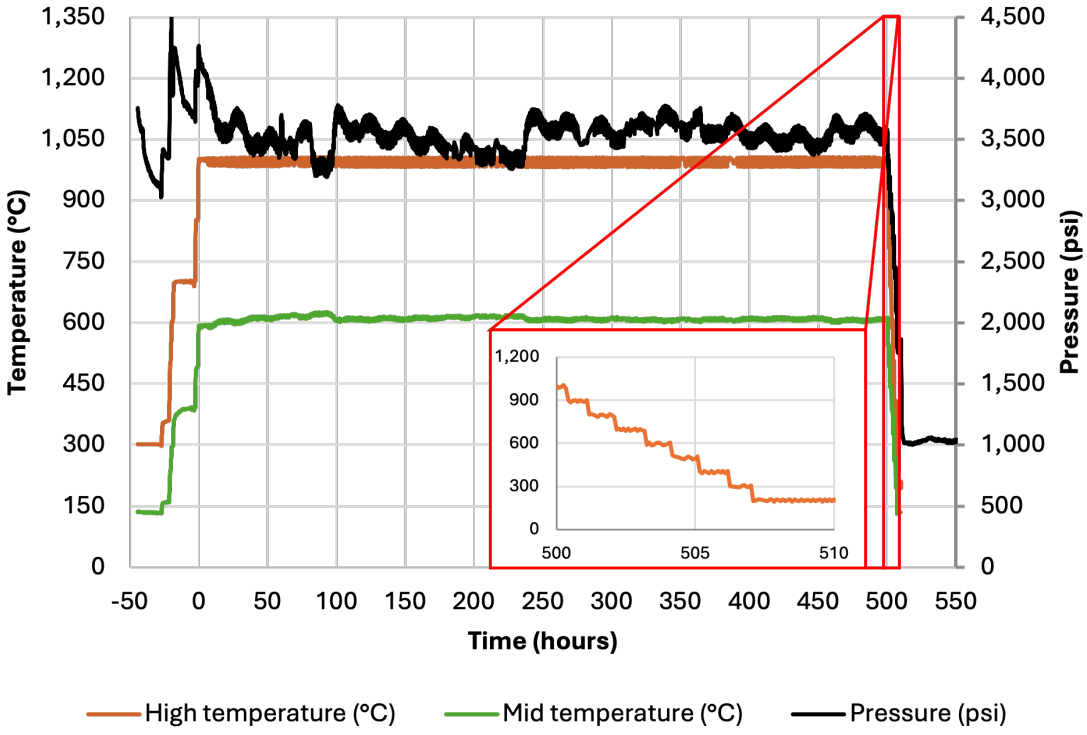

Figure 5. Measured temperature and pressure during the second 500 hours exposure. The insert shows the controlled cool down at 100 °C per hour.

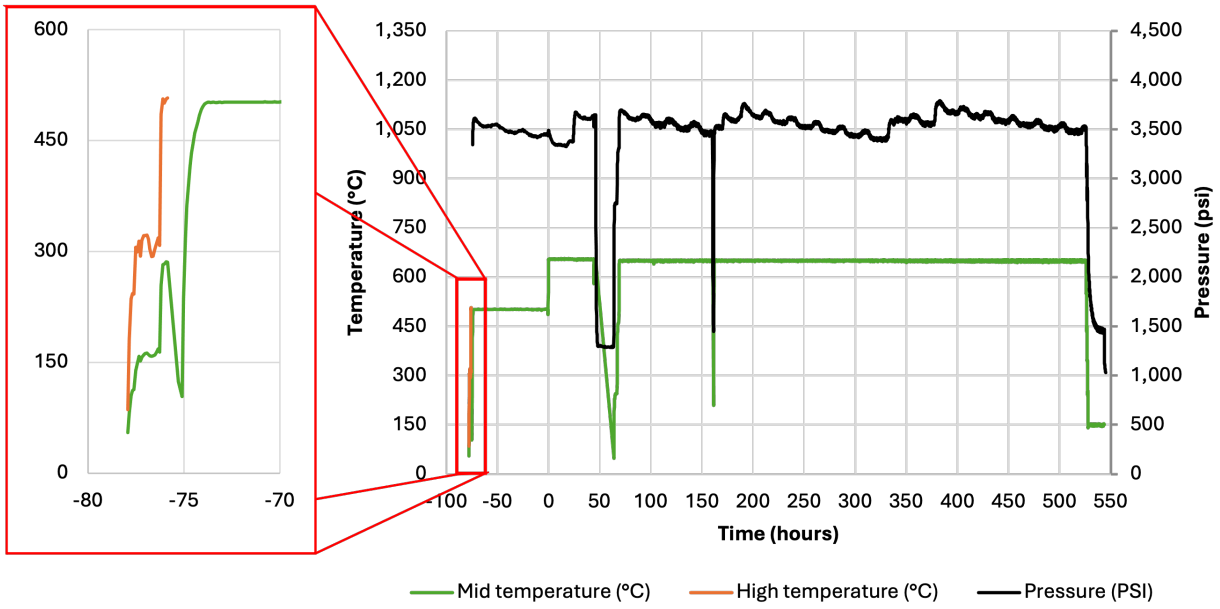

Figure 6. Measured temperature and pressure during the third and last 500 hours exposure. The insert shows the difference between the two thermocouples and when the high temperature thermocouple failed.

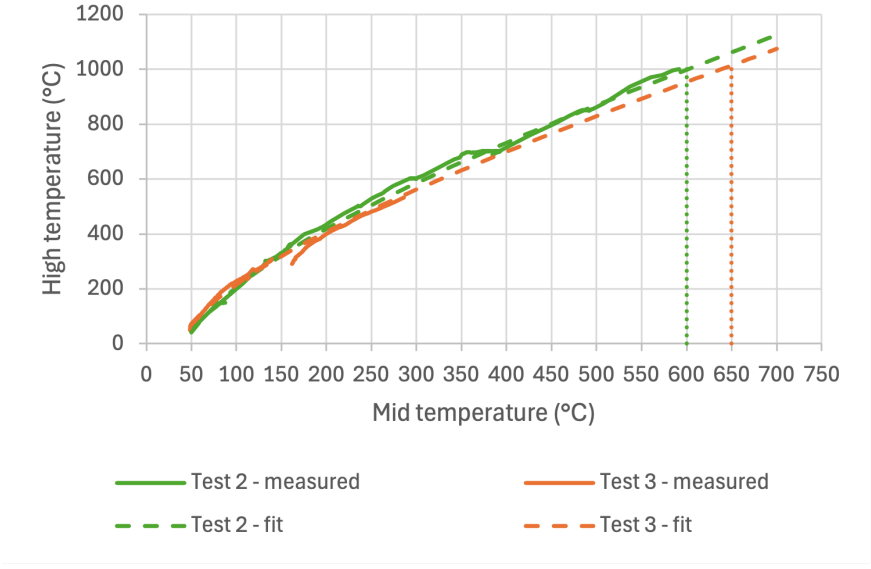

Figure 7. Comparison of the measured and logarithmic fit of the high and mid temperatures for test 2 and 3.

Table 2. Average and standard deviation of the high and mid temperatures collected during the three tests. Data when the induction heater stopped during the test was not included.

Test	High temperature		Mid temperature	
	Average (°C)	Standard deviation	Average (°C)	Standard deviation
1	1,031	41	882	46
2	995	7	609	5
3	-	-	650	2

The weight measurements were used to derive weight change per area, and oxidation rates. The mass change data as a function of the bare alloys are presented in Figure 8. Overall, mass changes were more significant for the nickel alloys than for the ferrous alloys and during the first two exposures. Mass changes were low for all alloys during the last exposure. Negative mass changes were observed during the second exposure on alloys 353 and APMT Kanthal, and during the third exposure on alloys 625 and APMT Kanthal. These mass losses indicate that the oxide was not stable.

The effect of the nanocrystalline bond coat is presented in Figure 9. The data are plotted on linear and log scale. The benefits of the bond coat are evident. Mass changes decreased drastically even on materials that displayed the highest mass changes, such as the nickel alloys during the first and second exposures. Benefits were also noticeable when the mass change of the bare materials were below 0.5 mg/cm^2 (the ferrous alloys during the second exposure and all alloys during the third exposure). It is also noticeable that some mass loss shifted to mass gain in the presence of the coating (alloy 353 during the second exposure and alloy APMT Kanthal during the second and third exposure). The coating only appeared to be detrimental for alloys 740H and 282 during the third exposure as their mass changes shifted from gains to losses.

The oxidation rates were calculated for all specimens during each interim and are presented as a function of time in Figure 10. The data is separated into four graphs for the bare alloys, the alloys with the nanocrystalline bond coat, the alloys with the nanocrystalline bond coat and the TBC, and the alloys with thermal spray bond coat and the TBC. Oxidation rates were usually highest on the bare alloys, on the nickel alloys, and during the second exposure. It can also be noted that the oxidation rates of the nickel alloys with the nanocrystalline bond coat decreased when the TBC was added. Furthermore, oxidation rates in the presence of TBC were lower when the bond coat was nanocrystalline instead of thermal sprayed. The largest mass change was observed on the alloy 282 with the thermal spray bond coat and the TBC during the third exposure. Photographs of those specimens are showed in Figure 11 after each exposure. The TBC was heavily degraded during the third exposure, especially near the edges of the specimens. The bond coat can be visible on some of those edges. Therefore, the observed mass loss is due to the TBC disbondment.

Results after the first exposure were compared to published data at 300 bar and 700 °C to

800 °C, see Figure 12. The rankings of the alloys as well as the trend with increasing temperature were similar between the two studies. This indicates that the induction heater in the autoclave could successfully be used to test materials in environments such as those found in oxy-combustion turbines using sCO_2.

This study of materials considered for oxy-combustion turbines in sCO_2 resulted in multiple findings:

- An induction heater placed in an autoclave can be successfully used to evaluate materials oxidation at pressure and at temperature exceeding 1,000 °C.
- Bare nickel alloys were more susceptible to oxidation than the ferrous alloys. However, the mechanical properties of the ferrous alloys are expected to be significantly worse at 1,000 °C.
- The addition of a nanocrystalline MCrAlY bond coat alone was beneficial to all alloys.
- TBC was more susceptible to damages when a thermal spray MCrAlY bond coat was used instead of nanocrystalline MCrAlY bond coat.
- Oxidation rates increased significantly from 800 °C to 1,000 °C.

a)

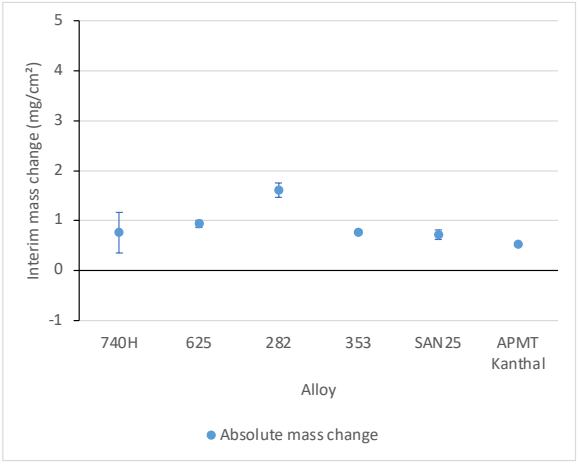

b)

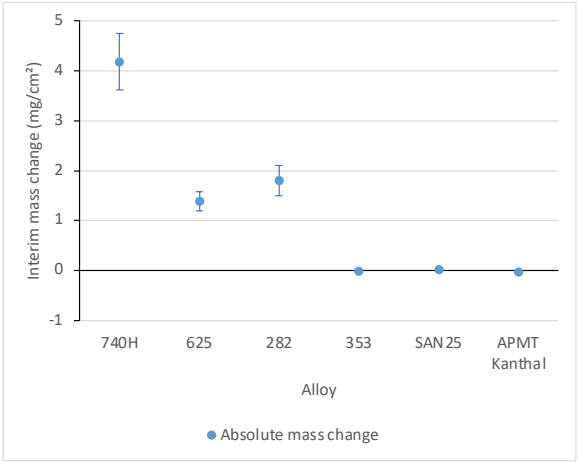

c)

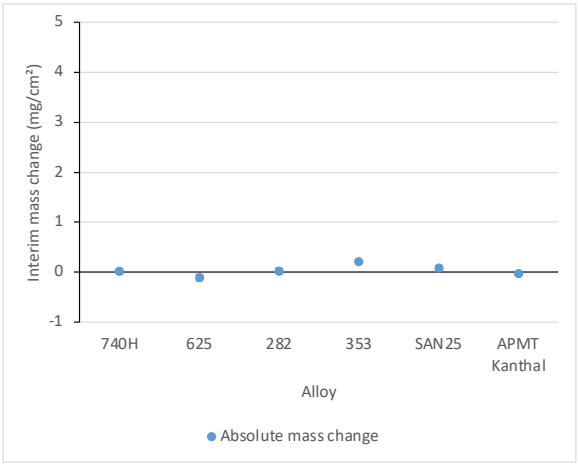

Figure 8. Mass change per area of the bare alloys during 500 hours after a) the first, b) second, and c) third exposure.

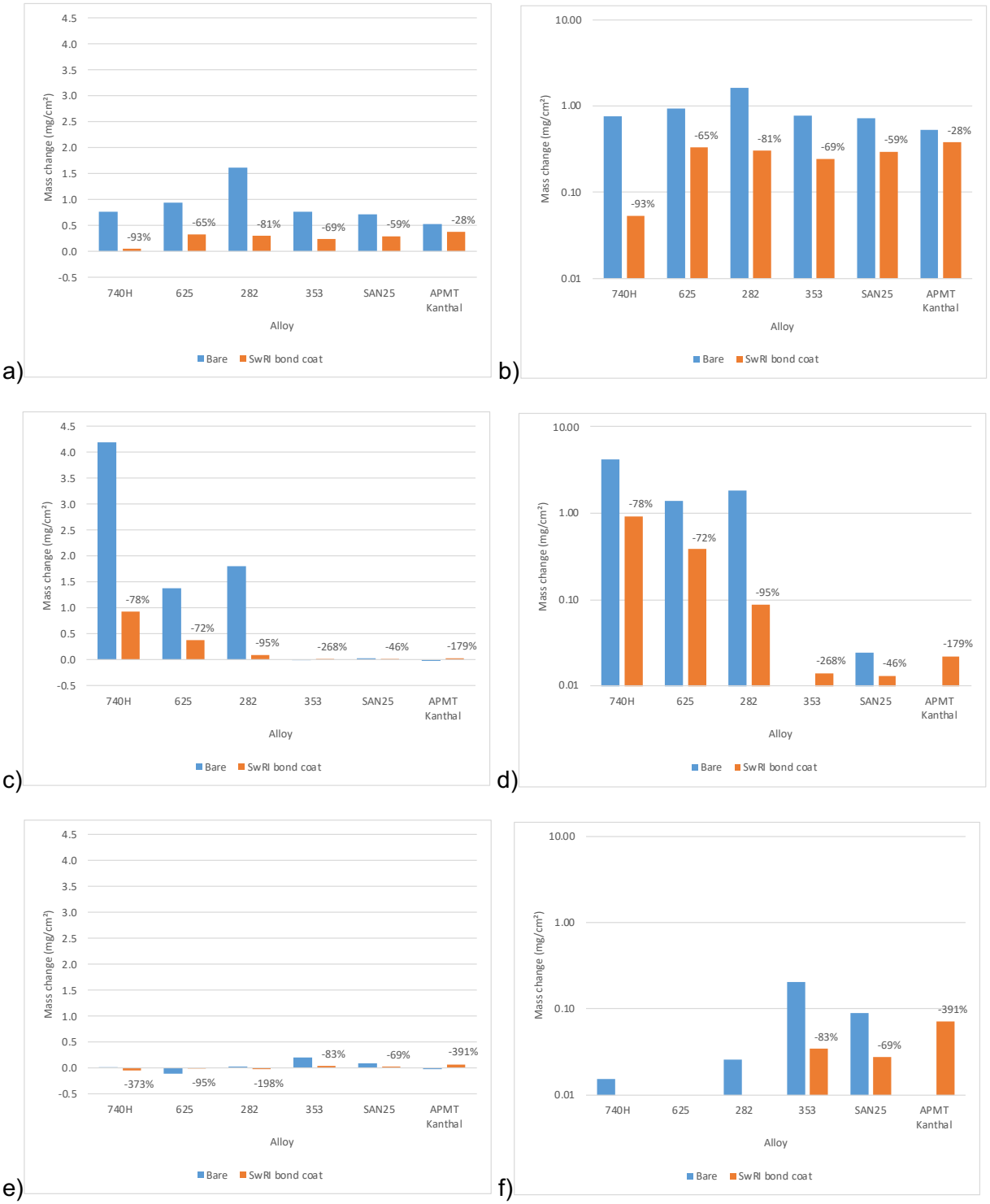

Figure 9. Mass change per area of the alloys with and without nanocrystalline MCrAlY coatings during 500 hours after a) and b) the first exposure, c) and d) the second exposure, and e) and f) the third exposure. Linear scales are used on the graphs a), c), and e). Logarithmic scales are used on graphs, b), d), and f). The percentage values indicate mass change variation between the bare and coated samples.

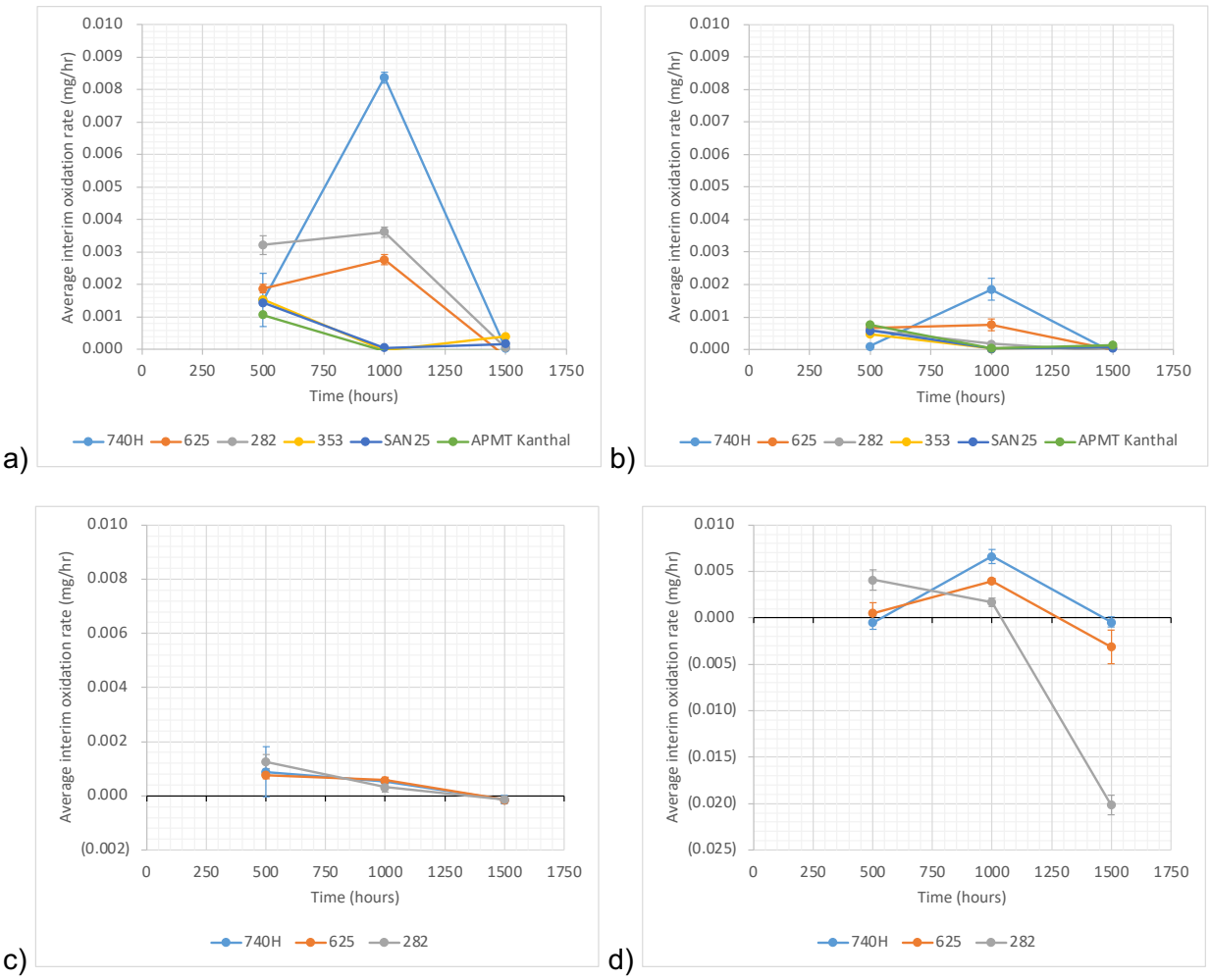

Figure 10. Interim oxidation rates as a function of time for a) the bare alloys, b) the alloys with the nanocrystalline MCrAlY coating, c) the alloys with nanocrystalline bond coat and TBC, and d) the alloys with thermal sprayed bond coat and TBC.

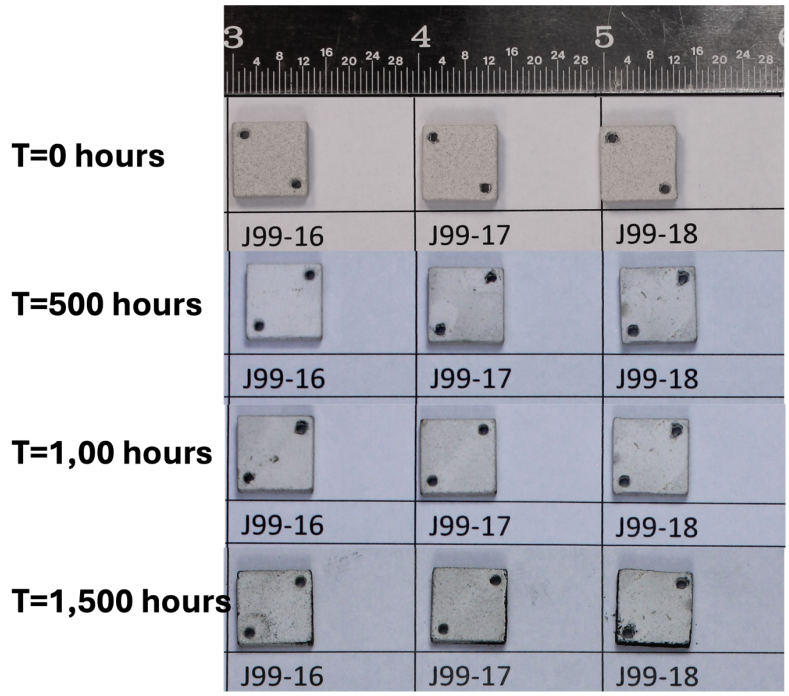

Figure 11. Photographs of the alloy 282 with thermal spray bond coat and TBC as received and after 500 hours, 1,000 hours, and 1,500 hours of exposure.

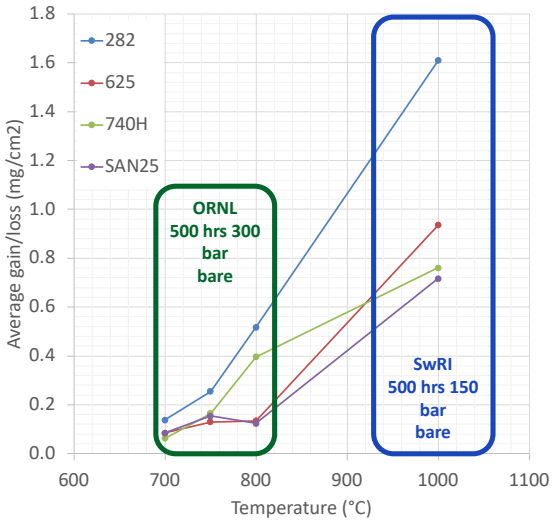

Figure 12. Comparison of average mass change after 500 hours at 1,000 °C and 150 bar in this study and at 700 °C to 800 °C at 300 bar measured during the DOE project CESL015 DE-EE0001556 performed at Oak Ridge National Laboratory.

REFERENCES

1. Weiland, N. T. & White, C. W. *Performance and Cost Assessment of a Natural Gas-Fueled Direct sCO_2 Power Plant*. NETL-PUB--22274, 1503567 http://www.osti.gov/servlets/purl/1503567/ (2019) doi:10.2172/1503567.

2. Goff, A., Lu, X. & Fetvedt, J. *Allam Cycle Zero Emission Coal Power*. (2020).

3. Moore, J. *et al.* Development of a 300 MWe Utility Scale Oxy-Fuel sCO2 Turbine. in *Proceedings of ASME Turbo Expo 2023* (Boston, MA, USA, 2023).

4. Pint, B. A. & Keiser, J. R. The Effect of Temperature on the sCO2 Compatibility of Conventional Structural Alloys. in *Proceedings of the 4th International Symposium on Supercritical CO2 Power Cycles.* (Pittsburgh, Pennsylvania, 2014).

5. Pint, B. A. & Thomson, J. K. Effect of Oxy-Firing on Corrosion Rates at 600–650 °C. *Materials and Corrosion* **65**, 132–140 (2014).

6. Pint, B. A., Brese, R. G. & Keiser, J. R. Effect of Pressure on Supercritical CO2 Compatibility of Structural Alloys at 750 °C. *Materials and Corrosion* **68**, 151–158 (2017).

7. Pint, B. A., Brese, R. G. & Keiser, J. R. Supercritical CO2 Compatibility of Structural Alloys at 400-750C. in *Corrosion 2016* (NACE International, 2016).

8. Kung, S. C. *et al.* Oxidation/Corrosion in Materials for Supercritical CO2 Power Cycles. in *Proceedings of the 5th International Symposium on Supercritical CO2 Power Cycles.* (San Antonio, TX, 2016).

9. Kung, S. C., Shingledecker, J. P., Wright, I. G. & Tossey, B. M. Oxidation and Carburization of Alloys Exposed to Impure Supercritical CO2. in *Corrosion 2017* (NACE International, 2017).

10. Cao, G., Firouzdor, V., Sridharan, K., Anderson, M. & Allen, T. R. Corrosion of Austenitic Alloys in High Temperature Supercritical Carbon Dioxide. *Corrosion Science* **60**, 246–255 (2012).

11. He, L.-F. *et al.* Corrosion Behavior of an Alumina Forming Austenitic Steel Exposed to Supercritical Carbon Dioxide. *Corrosion Science* **82**, 67–76 (2014).

12. Jelinek, J. J. *et al.* Corrosion Behavior of Alloys In High Temperature Supercritical Carbon Dioxide. in *Corrosion 2012* (NACE International, 2012).

13. Roman, P. J. *et al.* Corrosion Study of Candidate Alloys in High Temperature, High Pressure Supercritical Carbon Dioxide for Brayton Cycle Applications. in (NACE International, 2013).

Text here

ACKNOWLEDGEMENTS

This material is based upon work supported by the U.S. Department of Energy under Award Number DE-FE0031929.

The authors wish to acknowledge Justin Been (SwRI) for his assistance in building the high pressure and high temperature induction test setup and performing the testing, and Dustin Noll (SwRI) for his assistance in measuring and photographing the test specimens.

Ray Ariss, of Inductronix, is thanked for his continuous help and support in uniting the induction heater to the autoclave and in troubleshooting the entire system.

The assistance of Steve McCoy and Jack deBarbadillo of Special Metals, of Brett Tossey and Vinay Deodeshmukh of Haynes International, and of Luiza Esteves of Sandvik in providing the test materials is also acknowledged.

Plasma Technology, Inc. is recognized for the depositions of the thermal spray bond coat and the thermal barrier coatings.

DISCLAIMER